

# Silkworm Silk as an Engineering Material

J. PÉREZ-RIGUEIRO,<sup>1</sup> C. VINEY,<sup>2</sup> J. LLORCA,<sup>1</sup> M. ELICES<sup>1</sup>

<sup>1</sup> Departamento de Ciencia de Materiales, ETSI Caminos, Canales y Puertos, Ciudad Universitaria s/n, 28040 Madrid, Spain

<sup>2</sup> Department of Materials, University of Oxford, Parks Road, Oxford, OX1 3PH, Great Britain

Received 31 March 1998; accepted 9 May 1998

**ABSTRACT:** While silk exhibits high values of tensile strength and stiffness, these properties are compromised by their poor reproducibility. We present the results of experiments aimed at characterizing the variability of tensile properties exhibited by cocoon silk from *Bombyx mori* silkworms. Scanning electron microscopy is used to measure an average diameter for individual test specimens; the interspecimen variability of diameter is quantified and found to be inadequately represented by standard deviation. When load-extension data are converted into stress-strain curves, a marked improvement in reproducibility is realized if each specimen cross-section is calculated from diameter measurements specific to that specimen. Nevertheless, a significant variability in fracture stress remains; a Weibull analysis reveals that silkworm silk has a failure predictability comparable with that of glass and nonengineering ceramics. Unloading/reloading tests demonstrate that stiffness is not significantly affected by cumulative deformation, and the stress-strain relationship is not sensitive to strain rate. © 1998 John Wiley & Sons, Inc. *J Appl Polym Sci* 70: 2439–2447, 1998

**Key words:** silkworm silk; tensile test; fiber diameter; Weibull modulus

## INTRODUCTION

Biological materials often show a combination of properties that cannot be reproduced by artificial means. Silks, produced either by spiders or moth larvae, are a good example when compared with artificial organic fibers. Although it is possible to produce high-performance fibers (i.e., Kevlar 49) with a breaking strength above 3 GPa,<sup>1</sup> these fibers show an elongation to failure below 5%. On the other hand, natural silks have a lower strength ( $\approx 1$  GPa) but a higher elongation to failure (30%) (ref. 2 and references cited therein).

The principles that underlie these excellent properties are still largely unknown. It has long

been recognized that silkworm silk is made up of crystalline and noncrystalline regions,<sup>3</sup> and even more sophisticated models have been proposed for spider drag line silk (*Nephila clavipes*).<sup>4–6</sup> These models provide a qualitative basis for understanding the mechanical properties of the silk: the interconnected ordered regions would account for the stiffness of the material, whereas the disordered regions would account for the large elongation to failure. Meanwhile, reliable quantitative results have remained elusive, for two principal reasons: (1) silks are complex materials, whose detailed hierarchical microstructure is not easy to observe experimentally; and (2) silks show a large variability from sample to sample, so it is difficult to assign typical values even to common tensile properties.

The aim of this article is to address how variable the mechanical and geometrical features of silkworm (*Bombyx mori*) silk are, including vari-

Correspondence to: J. Pérez-Rigueiro (cm19@caminos.upm.es).

*Journal of Applied Polymer Science*, Vol. 70, 2439–2447 (1998)  
© 1998 John Wiley & Sons, Inc. CCC 0021-8995/98/122439-09

ations that could appear during our manipulation of the silk when preparing the samples. Although data on the mechanical properties of silkworm silk have already been published,<sup>7-9</sup> the present work focuses on the statistical aspects of this material's behavior. In particular, we demonstrate that silkworm silk has a Weibull modulus similar to that of glass. All the mechanical tests have been made with monofilament samples. In this context, monofilament means a have, which itself consists of two parallel fibroin subfilaments or brins. The two brins originate as solubilized fibroin within the worm's two silk glands. As fibroin leaves the glands, it is coated with another protein, sericin. The ducts leading from the glands merge before the silk reaches the single spinneret, so that a single have is spun. In addition to joining the brins, sericin sticks the have to already-spun material, ensuring the integrity of the cocoon.

The correct description of the geometry of the silk is not trivial.<sup>10</sup> Therefore, a statistical analysis has been made to determine how variable the fiber diameter is. This result is used later to convert force-displacement measurements into stress-strain curves.

Loading-unloading tests have been performed to explore how the tensile properties of the fibers are modified by cold drawing. Finally, because strain *rate* can influence the mechanical properties due to the viscoelastic properties of silk,<sup>11</sup> tests have been performed to determine its effect.

## EXPERIMENTAL

Silkworm cocoons (*Bombyx mori*) were boiled for 20 min in distilled water with no detergent or other additive. Fibers 15–25 cm long were obtained by pulling gently, taking care that they were not stressed plastically during this process. The fibers were allowed to dry overnight in air before performing any mechanical test. Typical relative humidity of the air in the laboratory was 50%.

The original fibers were cut into shorter lengths (6 cm) to prepare samples for the mechanical tests. The fibers were glued (Loctite 401) onto cardboard supports as shown in Figure 1. The cardboard was fixed in an Instron 4411 mechanical testing machine; cuts were made along the discontinuous lines shown in Figure 1, so that the load was transmitted through the fiber. Because the compliance of the fiber has been estimated as

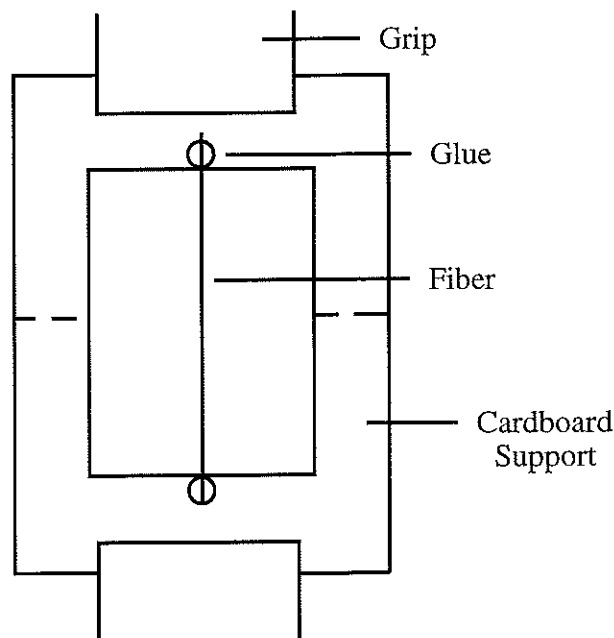


**Figure 1** Experimental setup for the tensile tests. The cardboard is cut with scissors through the discontinuous line before starting the experiment. The hole is 50 mm long.

3 orders of magnitude lower than that of any other part of the system, the displacement of the crosshead (resolution  $\pm 10 \mu\text{m}$ ) can be considered an accurate measurement of strain. Instead of a conventional load cell, a balance (Precisa 6100 C, resolution  $\pm 10 \text{ mg}$ ) was placed below the lower grip, and the force exerted on the fiber was determined from the decrease of initial weight measured. A strain rate of  $0.00017 \text{ s}^{-1}$  ( $0.01 \text{ min}^{-1}$ ) has been used unless otherwise stated.

The fibers were recovered after the test for the measurement of their diameter. Three small pieces (5 mm long) were cut from different parts of the tested fiber and metallized with gold before their introduction in the scanning electron microscope (JEOL 6300). The samples were observed at 10 kV, with a current of 0.6 nA. It has been assumed that neither the metallization nor the observation conditions in the microscope influences the geometry of the fibers.<sup>10</sup> Images were recorded on Polaroid film.

## RESULTS AND DISCUSSION

### Geometry of the Silk

Measurement of the geometrical parameters that describe the silk is a difficult task for three rea-

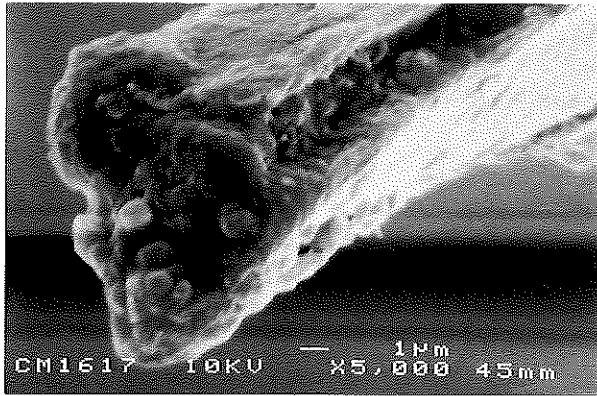


**Figure 2** Cross-section of *Bombyx mori* cocoon fiber is not always circular, as demonstrated by the approximately triangular cross-section shown in this micrograph of a single brin.

sons. First, the cross-section of neither brin nor bave is necessarily circular. Triangular and oval cross-sections have been found with a similar frequency as circular ones. An example of a triangular section is shown in Figure 2. Second, there is a significant variation of the fiber diameter along the fiber, due to the way in which the silk is produced through an active spinneret. Finally, the two-brin structure of native silk renders difficult the interpretation of data obtained by laser diffractometry as a measure of the diameter.<sup>10,12</sup> This last point has important practical consequences, because the alternative approach of using scanning electron microscopy is much slower, and the acquisition of enough data becomes a time-consuming process.

Nevertheless, the determination of stress-strain plots does require a value for the cross-sectional area. Faced with the difficulty of measuring a variable cross-sectional area directly, we make the significant simplification of treating each brin as a cylinder. We calculate mean bave area from measurements of brin diameter, recognizing that this will introduce a systematic error (but not a random error) into our estimates of

stress. This consistent method of obtaining sample cross-sections is not then itself a source of the variability in our results. We also recognize that the conversion of brin diameter to bave cross-sectional area ignores any possible contribution of residual sericin to the mechanical properties of the bave; however, this is consistent with standard practice. The mean brin diameter was estimated from micrographs taken of different parts of the fiber. At least three different regions in each fiber were photographed to sample the variation along it. Two different orientations ( $0-50^\circ$ ), obtained by rotating the sample around its axis in the microscope, were used to estimate an apparent diameter. (Ideally  $0-90^\circ$  should have been used, but this was beyond the geometrical capabilities of the microscope.) Over 80 photographs were taken in our study of 14 samples. The results of this study are presented in Table I.

The mean diameter obtained from these data is  $11.5 \mu\text{m}$ . A variation of  $\sim 18\%$  ( $2.1 \mu\text{m}$ ) can result from observing the same section of the brin at  $0^\circ$  and  $50^\circ$ . The greater  $D_o - D_{50}$  standard deviation compared with the diameter standard deviation is a consequence of having twice as many data for the determination of the diameter than for the determination of  $D_o - D_{50}$ . Instead of using the standard deviation as a measurement of the variation of the diameter, Figure 3 shows the cumulative probability of finding a brin with a mean diameter smaller than or equal to  $D$ . If the standard deviation in Table I is considered naively, it could appear that the mean diameters of brins group very close to the central value ( $11.5 \mu\text{m}$ ). Figure 3, however, shows how a significant number of brins are several microns thicker or thinner than this central value. Even worse, there is a  $>100\%$  difference between the minimum and maximum value. Consequently, properties that depend on details rather than on mean values of specimen cross-section (i.e., ultimate tensile strength) must show a large spread of values.

**Table I** Statistics of the Apparent Diameter of *Bombyx mori* Silk Brin

Mean Brin Diameter ( $\mu\text{m}$ )	Standard Deviation ( $\mu\text{m}$ )	Mean Difference of the Diameter $ D_o - D_{50} $ ( $\mu\text{m}$ )	Standard Deviation $ D_o - D_{50} $ ( $\mu\text{m}$ )	Max $D$ ( $\mu\text{m}$ )	Min $D$ ( $\mu\text{m}$ )
11.5	0.2	2.1	0.4	16.7	6.8

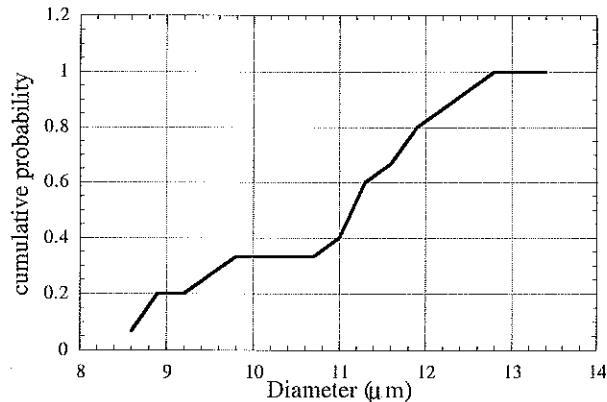


**Figure 3** Cumulative probability of finding a fiber with a diameter smaller than or equal to  $D$ .

### Tensile Tests on Silk

The force-strain results of the tensile tests performed on 11 different fibers are showed in Figure 4. The original length of the fibers was  $L_0 = 50$  mm, and the nominal strain has been calculated, using the original length, as  $\varepsilon = \Delta L/L_0$ . The large spread of the data is evident, not only concerning the ultimate tensile strength, but also the overall force-strain plot.

The spread of the data is reduced drastically when adjacent samples cut from the same original fiber are compared. In this case, the force at any plastic strain shows  $<10\%$  variation (as illustrated in Figure 5, where four tests on adjacent samples are shown), compared with the  $>200\%$  difference across all the samples. The relatively good reproducibility of the mechanical properties of adjacent samples has long been recognized in

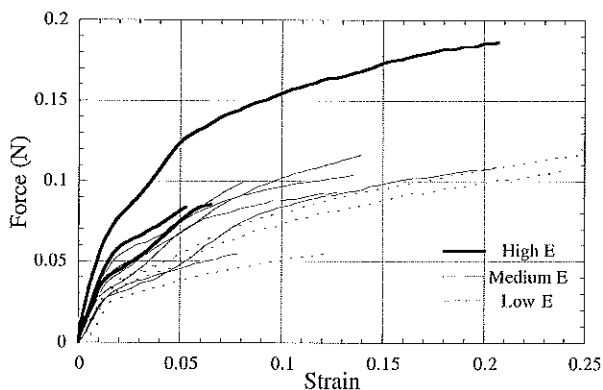


**Figure 4** Force-strain characteristics of silkworm silk. The designations “high  $E$ ,” “medium  $E$ ,” and “low  $E$ ” refer to the classification of these results that is possible after force has been rescaled as stress (Fig. 6).

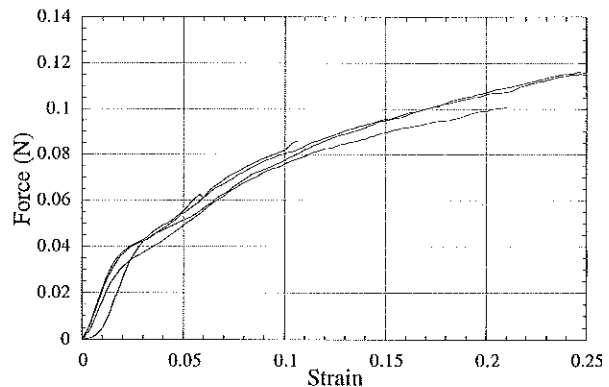


**Figure 5** Comparison of force-strain plots of four adjacent specimens obtained from the same original fiber. Observe the decrease of data scatter compared with Figure 4.

the context of spider dragline silk,<sup>13</sup> where adjacent samples are more easily prepared. The difference in ultimate tensile strength of adjacent samples is not usually  $>10\%$ , although some differ by  $>50\%$ . Both results can be explained from a statistical point of view: the force-strain plots depend on mean values (i.e., mean diameter), which are likely to be similar in adjacent samples, whereas tensile strength is greatly influenced by the presence of defects.

Although the use of the *overall* mean diameter would provide a working basis for rescaling force as stress, no improvement would be obtained in reducing the spread of the data. Therefore, a mean diameter has been calculated for *each individual* fiber, and the corresponding stress-strain plots are shown in Figure 6. It is worth remarking that the apparent bave area calculated from the

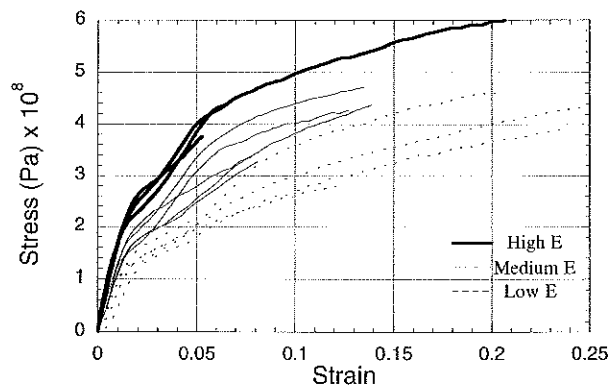


**Figure 6** Stress-strain characteristics of silkworm silk (stress calculated using average brin diameter in each sample).

**Table II Elastic Modulus and Yield Stress of *Bombyx mori* Silk**

	“Low” Elastic Modulus	“Medium” Elastic Modulus	“High” Elastic Modulus
Elastic modulus (GPa)	$8.9 \pm 0.5$	$12.8 \pm 0.7$	$17.4 \pm 0.4$
Yield stress (MPa)	$126 \pm 9$	$142 \pm 9$	$231 \pm 14$

mean brin diameter does not correspond to the initial area, because the geometrical measurements have been obtained from plastically deformed samples. The initial area is needed to determine the nominal stress, and it can be calculated assuming that the sample volume remains constant throughout the test. In this case, the initial area is given approximately by:

$$A_o = \frac{A_f l_f}{l_o} \quad (1)$$

where  $A_o$  is the initial area,  $A_f$  is the final area (calculated from the apparent diameter),  $l_o$  is the initial length, and  $l_f$  is the final length of the fiber.

The spread of the data is reduced from 200% for the raw force-strain curves (Fig. 4) to 70% for the stress-strain curves (Fig. 6). This indicates that the procedure used to obtain the mean diameter can improve the reproducibility of the results. From the plots presented in Figure 6, it is possible to obtain the mechanical properties of the silk, such as the elastic modulus and the yield stress, with the latter being calculated conventionally as the stress at 0.2% deformation. The elastic modulus can be used to classify all the tests in three different groups, which are indicated in the plot. The mechanical properties for each group are shown in Table II.

We believe that the condition of the sericin coating is responsible for these differences, as will be explained in greater detail in a subsequent publication.<sup>14</sup> Our choice of three distinct categories for classifying fibers according to their modulus is justified by two considerations. The differences between the corresponding values of mean elastic modulus are large, compared with the values of standard deviation. Also, the same grouping of results can be achieved by considering yield stress instead of initial modulus, so we are confident that the classification reflects real material differences. Literature values of modulus,<sup>9</sup> for samples of *Bombyx mori* silk tested at a comparable strain rate and also assumed to be cylindri-

cal, are close to 5 GPa. The fact that our values for modulus are consistently higher than these must reflect our efforts to obtain a representative cross-sectional area for each individual sample tested, because our ability to measure loads and displacements accurately is comparable to that of previous researchers.

As an alternative to using the mean diameter to calculate a representative cross-sectional area, we also explored the consequences of calculating final area from the *minimum* diameter of each sample. We were motivated by the possibility that thinner regions of the sample might also be where the deformation is localized—in other words, the possibility that the thinner regions might dominate the overall response of the fiber to loading. However, Figure 7 shows a marked increase in the spread of the data relative to the original force-strain curves (Fig. 4). The implication is that stress concentration at microstructural flaws, rather than at geometrically thinner regions, dominates the deformation and eventual failure of the silk. This conclusion is borne out by the low Weibull modulus of this material, as measured below.

From the previous discussion, an even larger scatter in the data is expected when studying the

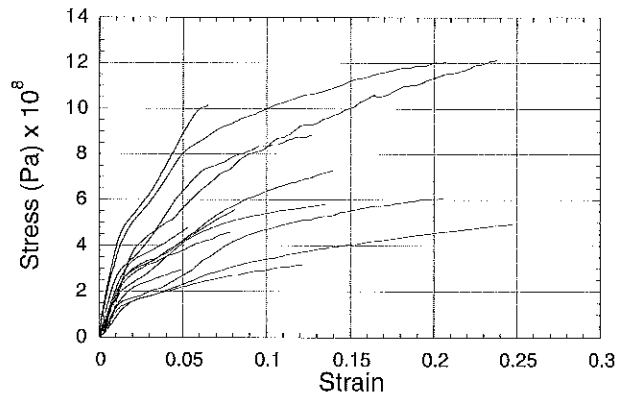


**Figure 7** Stress-strain characteristics of silkworm silk (stress calculated using smallest measured brin diameter in each sample).

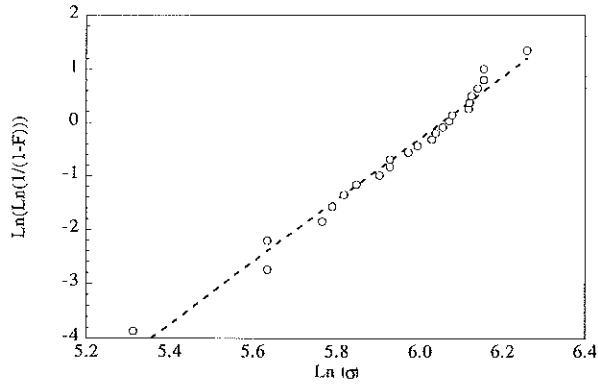


**Figure 8** Determination of the Weibull parameters of silk.

ultimate tensile strength of the fibers. Over 25 tests on 50-mm-long fibers have been done to obtain statistically significant results. The scatter of the data was just below 300%, and no difference could be observed between fibers with low and medium elastic modulus.

These large variations are very often found when studying artificial fibers, such as carbon or silicon carbide (Nicalon), and the usual way to analyze them is through Weibull statistics.<sup>15,16</sup> In Weibull's theory, the probability of fracture in a fiber is given by:

$$F = 1 - \exp\left(-\frac{L}{L_0}\left(\frac{\sigma}{\sigma_0}\right)^m\right) \quad (2)$$

where  $m$ ,  $\sigma_0$ , and  $L_0$  are parameters characteristic of the material. In this case, because all of the tested fibers had the same length, eq. (1) becomes:

$$F = 1 - \exp\left(-\left(\frac{\sigma}{\sigma_0}\right)^m\right) \quad (3)$$

or equivalently:

$$\text{Ln}\left(\frac{1}{1-F}\right) = \left(\frac{\sigma}{\sigma_0}\right)^m \quad (4)$$

If  $\text{Ln}(\text{Ln}(1/(1-F)))$  is plotted versus  $\text{Ln } \sigma$ , a straight line is obtained, with slope  $m$  and extrapolated intercept  $-m \text{Ln } \sigma_0$ . The result of applying this analysis to the silk fibers is shown in Figure 8. Tests of the high elastic modulus fibers are not included because they seem to lie on a different line; this observation can also be ascribed to the presence of sericin.<sup>14</sup> The data have

been fitted using a least-squares method with a correlation  $r = 0.989$ . From this plot, it can be concluded that *Bombyx mori* silk fibers obey Weibull statistics with values of  $m = 5.76 \pm 0.01$  and  $\sigma_0 = 403 \pm 1$  MPa. The low value of its Weibull modulus ranks silk alongside glass ( $m \approx 4.8$ ) and common ceramics ( $5 < m < 25$ )<sup>17</sup> in regard to the poor reproducibility of its breaking strength. Therefore, although silkworm silk exhibits a unique combination of high strength, stiffness, and toughness as previously noted, the poor reproducibility of its tensile properties may limit the engineering applicability of single fibers. An improvement in reproducibility can be expected from fiber that is spun at a fixed rate from solutions of recombinant silk-like protein under controlled conditions through a passive spinneret. We also note that Weibull modulus and reproducibility are of little consequence to the silkworm, because the fiber is laid down to build up a dense mat in which the sericin binder promotes load transfer across the entire structure. It will be interesting to determine whether spider drag line, where dependable properties are required from single fibers, has a higher Weibull modulus for fracture than silkworm silk.

### Unloading/Reloading Tests

Given the difficulty of handling single silk fibers without accidentally introducing deformation, we performed unloading/reloading tests to see whether mechanical properties are sensitive to previous stretching. The experimental setup was similar to that used for the simple tensile tests.

Figure 9 corresponds to an unloading/reloading

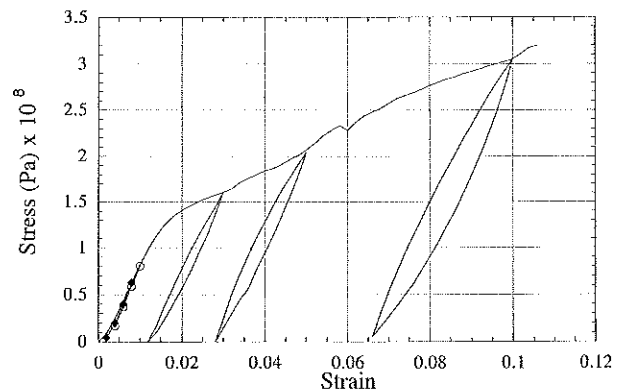


**Figure 9** Tensile test with four unloading/reloading steps (the first unloading/reloading step is superimposed on the initial elastic zone and marked with symbols).

**Table III Elastic Modulus of the Initial Loading Step and Subsequent Reloading Steps**

	Initial Load	1st Reload	2nd Reload	3rd Reload	4th Reload
$E$ (GPa)	8.2	8.2	8.6	8.7	8.9

test with four unloading/reloading steps. The steps were chosen so that the first was performed before the yield point was reached and the rest after passing it. The last step was performed just below the ultimate tensile strength. From these data, it is evident that there is a *true* elastic zone before reaching a yield point, at least at and around the strain rate of  $0.00017 \text{ s}^{-1}$  considered (see herein); the fiber can be stretched up to this point during manipulation without introducing permanent deformation or changing the elastic modulus.

Permanent deformation is introduced if the fiber is stretched beyond the apparent yield point, confirming that yield has indeed occurred. Hysteresis effects due to the viscoelastic properties of silk are now evident during the unloading/reloading process. The nonlinear stress-strain relationship during unloading precludes accurate measurement of elastic modulus; the viscoelastic effects are more apparent during unloading than during reloading. The elastic modulus for reloading can be measured directly from the plot. As can be seen in Figure 9 and Table III, the elastic modulus on loading/reloading is not sensitive to plastic deformation; in other words, stretching the fiber beyond its yield point and unloading is simply equivalent to expanding the elastic range of the fiber up to the new yield point, but neither the elastic modulus nor the overall shape of the plot up to its ultimate tensile strength are affected. If samples were to be stretched accidentally during handling (e.g., while being removed from the cocoon or mounted on the tensometer), it is likely that such deformation would occur at rates far greater than those studied herein, providing even less opportunity for viscous flow. Because the tensile modulus shows no sensitivity to significant plastic deformation, or to strain rate (see below), we are confident that measurement of cross-sectional area does indeed represent the greatest source of error in modulus characterization.

At microstructural and molecular scales, changes that occur upon deformation and in-

crease tensile modulus must be offset by changes that decrease the modulus. For example, both increased chain alignment in amorphous regions and enhanced relative alignment of crystalline regions would lead to a higher modulus, but simultaneous destruction of crystalline regions would lead to a lower modulus. Detailed modeling and microstructural studies are needed to characterize the competition between these processes.

### Influence of the Strain Rate

The viscoelastic behavior of silk<sup>11</sup> implies that the measured mechanical properties should depend on the strain rate; therefore, it is necessary to check whether a result obtained at a given strain rate is valid at a different strain rate. Necessarily, tests performed at different rates have to be performed on different specimens. The observed variability in the mechanical properties of silk may therefore not allow us to obtain clear conclusions when comparing tests on different specimens, because the intrinsic scatter of the data is so large. Fortunately, the comparative reproducibility of measurements made on *adjacent* samples cut from a given thread, as noted previously, allows us to obtain some information on how strain rate influences the behavior of silk.

Tests at strain rates of  $0.000017 \text{ s}^{-1}$ ,  $0.00017 \text{ s}^{-1}$  (the strain rate chosen for all the previous tensile tests) and  $0.00090 \text{ s}^{-1}$  were performed, and the results of these tests on adjacent samples from an original thread are shown in Figure 10. From these results, it seems that the mechanical properties are insensitive to the strain rate in a range of nearly 2 orders of magnitude. This observation is consistent with results obtained from

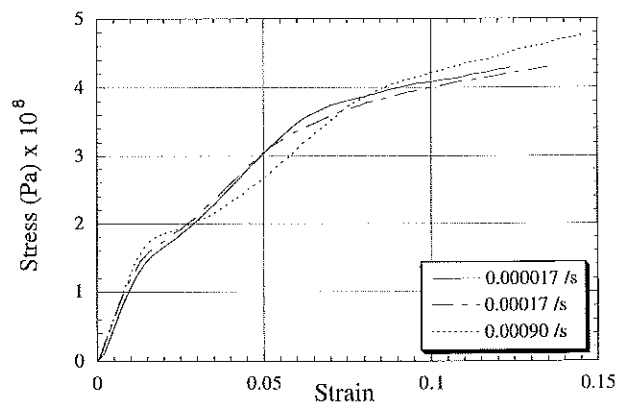


**Figure 10** Strain rate does not significantly influence the stress-strain characteristics in the range studied.

spider drag line,<sup>18</sup> which exhibits little difference in stress-strain behavior at quasistatic and ballistic strain rates. The absence of significant viscous creep in the response of both materials is consistent with the tests being conducted at temperatures far below the principal glass transition ( $\sim 175^\circ\text{C}$  for *Bombyx mori* silk<sup>19</sup> and  $160^\circ\text{C}$  for spider drag line<sup>20</sup>).

## SUMMARY AND CONCLUSIONS

### Diameter

We demonstrate that the brin produced by *Bombyx mori* silkworms has a highly nonuniform cross-sectional geometry, with respect to both shape and absolute dimensions. Standard deviation is not necessarily the best indicator of the large variability in mean diameter. The spread is more effectively represented by considering the cumulative success of finding samples with a mean diameter less than or equal to a given value.

### Elastic Modulus

The variability in data obtained from tensile tests can be reduced by (1) testing adjacent samples cut from the same original fiber and (2) calculating an average cross-sectional area for each individual sample tested. Samples can be classified into three distinct groups according to the value of their initial elastic modulus. The same classification can be achieved with reference to yield stress. We believe that these differences result from differences in the condition of the sericin coating.

### Tensile Strength

The scatter in tensile fracture strength is even more pronounced than the scatter in elastic modulus, depending not only on the variability in cross-sectional area, but also on the distribution of microstructural flaws. The fracture strength of low- and medium-stiffness fibers follows the same Weibull plot. The Weibull modulus of *Bombyx mori* silk is similar to that of glass and common ceramic materials. Despite its attractive combination of strength, stiffness, and toughness, natural silk has the failure predictability of a brittle material. It is expected that silk synthesized by genetically modified bacteria and spun under controlled conditions through an artificial spinneret will have a more uniform cross-sectional area,

reproducible molecular alignment, and fewer microstructural flaws; such material should exhibit improved reliability as an engineering material.

### Unloading/Reloading Tests and Effect of Strain Rate

In tensile tests ( $0.00017\text{ s}^{-1}$ ) where the experiment is interrupted by unload/reload steps, the tensile modulus on reloading is insensitive to the cumulative deformation experienced by the specimen. The stress-strain relationship is also found to be insensitive to strain rate. Measurements of tensile modulus should therefore not be prejudiced by accidental stretching introduced during specimen handling. Microstructurally, deformation mechanisms that increase tensile modulus (e.g., increased alignment of chains) must be balanced by at least one mechanism that decreases tensile modulus (e.g., breakup of crystalline regions).

We are indebted to Dr. Marion Goldsmith (University of Rhode Island) for kindly providing a supply of *Bombyx mori* cocoons.

## REFERENCES

1. A. R. Bunsell, *Encyclopedia of Applied Physics*, Vol. 16, 1996, p. 343.
2. C. Viney, *Mater. Sci. Eng. R*, **10**, 187 (1993).
3. R. E. Marsh, R. B. Corey, and L. Pauling, *Biochim. Biophys. Acta*, **16**, 1 (1955).
4. B. L. Thiel, K. B. Guess, and C. Viney, *Biopolymers*, **41**, 703 (1997).
5. B. L. Thiel and C. Viney, *J. Microsc.*, **185**, 179 (1997).
6. A. H. Simmons, C. A. Michal, and L. W. Jelinski, *Science*, **271**, 84 (1996).
7. Y. Kawahara, M. Shioya, and A. Takaku, *J. Appl. Polym. Sci.*, **61**, 1359 (1996).
8. G. Freddi, M. R. Massafra, S. Beretta, S. Shitaba, Y. Gotoh, H. Yasui, and M. Tsukada, *J. Appl. Polym. Sci.*, **60**, 1867 (1996).
9. D. L. Kaplan, S. J. Lombardi, W. S. Muller, and S. A. Fossey in *Biomaterials*, D. Byrom, Ed., Stockton Press, New York, 1991, p. 1.
10. D. L. Dunaway, B. L. Thiel, and C. Viney, *J. Appl. Polym. Sci.*, **58**, 675 (1995).
11. K. M. Parthasarathy, M. D. Naresh, V. Arumugam, V. Subramanian, and R. Sanjeevi, *J. Appl. Polym. Sci.*, **59**, 2049 (1996).
12. J. V. Brancik and A. Datyner, *Textile Res. J.*, **October**, 662 (1977).
13. R. W. Work, *Textile Res. J.*, **47**, 650 (1977).



14. J. Pérez-Rigueiro, C. Viney, J. Llorca, and M. Elices, to appear.
15. T.-W. Chou, *Microstructural Design of Fiber Composites*, Cambridge University Press, Cambridge, 1992, p. 98.
16. G. Simon and A. R. Bunsell, *J. Mater. Sci.*, **19**, 3949 (1984).
17. *Materials for Engineering*, B. Derby, D. Hills, and C. Ruiz, Eds., Longman Scientific and Technical, 1992, p. 225.
18. P. M. Cunniff, S. A. Fossey, M. A. Auerbach, and J. W. Song, in *Silk Polymers. Materials Science and Biotechnology*, D. L. Kaplan, W. W. Adams, B. L. Farmer, and C. Viney, Eds., ACS Symposium Series, ACS, Washington, DC, 1994, p. 234.
19. S. Nakamura, J. Magoshi, and Y. Magoshi, in *Silk Polymers. Materials Science and Biotechnology*, D. L. Kaplan, W. W. Adams, B. L. Farmer, and C. Viney, Eds., ACS Symposium Series, ACS, Washington, DC, 1994, p. 211.
20. K. B. Guess and C. Viney, *Thermochim. Acta*, **315**, 61 (1998).

